Modeling gross primary production of alpine ecosystems in the Tibetan Plateau using MODIS images and climate data

Zhengquan Li [a,b], Guirui Yu [a,*], Xiangming Xiao [c], Yingnian Li [d], Xinquan Zhao [d], Chuanyou Ren [a], Leiming Zhang [a], Yuling Fu [a]

[a] Institute of Geographic Sciences and Natural Resources Research, Chinese Academy of Sciences, Beijing 100101, China
[b] Zhejiang Climate Center, Zhejiang Meteorological Bureau, Zhejiang 310017, China
[c] Institute for the Study of Earth, Oceans and Space, University of New Hampshire, Durham, NH 03824, USA
[d] Northwest Institute of Plateau Biology, CAS, Qinghai 810001, China

Abstract

The eddy covariance technique provides measurements of net ecosystem exchange (NEE) of CO_2 between the atmosphere and terrestrial ecosystems, which is widely used to estimate ecosystem respiration and gross primary production (GPP) at a number of CO_2 eddy flux tower sites. In this paper, canopy-level maximum light use efficiency, a key parameter in the satellite-based Vegetation Photosynthesis Model (VPM), was estimated by using the observed CO_2 flux data and photosynthetically active radiation (PAR) data from eddy flux tower sites in an alpine swamp ecosystem, an alpine shrub ecosystem and an alpine meadow ecosystem in Qinghai–Tibetan Plateau, China. The VPM model uses two improved vegetation indices (Enhanced Vegetation Index (EVI), Land Surface Water Index (LSWI)) derived from the Moderate Resolution Imaging Spectral radiometer (MODIS) data and climate data at the flux tower sites, and estimated the seasonal dynamics of GPP of the three alpine grassland ecosystems in Qinghai–Tibetan Plateau. The seasonal dynamics of GPP predicted by the VPM model agreed well with estimated GPP from eddy flux towers. These results demonstrated the potential of the satellite-driven VPM model for scaling-up GPP of alpine grassland ecosystems, a key component for the study of the carbon cycle at regional and global scales.
© 2006 Elsevier Inc. All rights reserved.

Keywords: Vegetation Photosynthesis Model; Eddy covariance; Light use efficiency; CO_2 fluxes

1. Introduction

Eddy covariance technique is one of the best micrometeorological methods for estimating the CO_2, water, and energy exchange between the atmosphere and terrestrial ecosystems. In recent years, many studies have used eddy covariance techniques to measure net ecosystem exchange of CO_2 (NEE), and the resultant NEE data provide valuable information related to photosynthesis period and gross primary production (GPP) of ecosystems (Falge, Baldocchi, et al., 2002a; Falge, Tenhunen et al., 2002b). However, flux tower sites only provide integrated CO_2 flux measurements over footprints with sizes and shapes (linear dimensions typically ranging from hundreds of meters to 1 km) that vary with the tower height, canopy physical characteristics and wind velocity (Osmond et al., 2004). Because of the large spatial heterogeneity and temporal dynamics of ecosystems across complex landscapes and regions, it is a challenging task to scale up those CO_2 flux measurements from site level to regional or global scale (Yu et al., 2005). Satellite remote sensing can provide consistent and systematic observations of vegetation and ecosystems, and has played an increasing role in characterization of vegetation structure and estimation of gross primary production (GPP) or net primary production (NPP) (Behrenfeld et al., 2001; Field et al., 1998; Ruimy et al., 1999; Running et al., 2000). Many studies aim to integrate flux tower data and remote sensing for regional carbon budget research (Aalto et al., 2004; Oechel et al., 2000; Turner et al., 2003).

Satellite remote sensing can be used to estimate either GPP or NPP, but is not capable of validating model-generated surfaces for

---

heterotrophic respiration and hence NEE (Running et al., 1999). On the other hand, although the eddy covariance techniques can directly measure NEE, and provide the best approach to calculate GPP of ecosystems, it still has a large uncertainty to estimate NPP because it is difficult to partition respiration of ecosystems into autotrophic respiration and heterotrophic respiration. GPP estimation is a juncture of integrating tower flux and remote sensing for the studies of regional vegetation productivity and carbon cycle. Recently, Xiao, Hollinger, et al. (2004a, Xiao, Zhang, et al., 2004b, Xiao, Zhang, Hollinger et al., 2005a, Xiao, Zhang, Saleska et al., 2005b) have developed the satellite-based Vegetation Photosynthesis Model (VPM) that estimates GPP of ecosystems, and they have successfully demonstrated the potential of the model for scaling-up GPP of forests at the CO_2 flux tower sites (temperate deciduous broadleaf forest, evergreen coniferous forest, and seasonally moist tropical forest). However, the VPM model has not been evaluated and applied in alpine grassland ecosystems. Validation of a new global model is a daunting task, as an ideal testing would be conducted across a full range of biome types and climate. In this study, our objective is twofold: (1) to examine biophysical performance of vegetation indices in relation to seasonal dynamics of CO_2 fluxes, and (2) to further evaluate the dependability of the VPM model for estimating GPP of alpine grassland ecosystems. The improved vegetation indices are derived from image data of Moderate Resolution Imaging Spectral radiometer (MODIS), onboard the NASA Terra satellite, collected in 2004. This study will help better understand the seasonal dynamics of CO_2 fluxes in the vast Qinghai–Tibetan Plateau (~ 2.5 million km^2), the roof-of-the-world, where natural vegetation is dominated by high-altitude arid and cold steppe and is sensitive to changes in climate and land use (e.g., livestock grazing). It will also explore the potential of satellite remote sensing for studying and monitoring vegetation and carbon fluxes in the Tibetan Plateau.

2. Materials and methods

2.1. Brief description of the study sites

The CO_2 eddy flux tower sites are located at the Haibei Alpine Meadow Ecosystem Research Station in Qinghai province, northwestern China. The Haibei station lies in a large valley surrounded by the Qilian Mountain at latitude 37°5′–37°9′N, and longitude 101°2′–101°4′E. The terrain is characterized as large-area flat plains with small hills, with elevation ranging from 3100–3400 m. It has a plateau continental climate, dominated by the southeast monsoon in summer and high pressure from Siberia in winter. The annual global solar radiation was up to 6000–7000 MJ/m^2. The annual mean air temperature was −1.7 °C, with a range from 27.6 °C to −37.1 °C. Annual precipitation ranges from 426 mm to 860 mm with a mean of 600 mm, mostly occurring from May to September (Zhao & Zhou, 1999). The study area is dominated by three major soil types: mat cryic cambisols (alpine meadow soil), mollic cryic cambisols (alpine shrub soil), and orthic spodosols (bog soil). Alpine meadow on the sunny slope of mountain and plain area is largely composed of *Kobresia*

Table 1
Location and characteristics of the three flux tower sites in Qinghai–Tibetan Plateau, China*

Site	Longitude (°E)	Latitude (°N)	Elevation (m)	Ecosystem type	Canopy height (m)	LAI	EC height (m)
BT	101.3050	37.6135	3148	Meadow	0.2	3.4	2.2~2.5
SD	101.3271	37.6088	3160	Swamp	0.4	3.5	2.2
GCT	101.3312	37.6654	3293	Shrub	0.5	2.8	2.2

* EC is Eddy covariance system, BT is alpine meadow ecosystem, SD is alpine swamp site, and GCT is alpine shrub site.

humilis, *Festuca ovina*, and *Elymus nulan*. Alpine shrub meadow on mountain shadow slopes is dominated by *Potentilla fruticos*, and its ground layer is large covered by *K. humilis*, *F. ovina*, and *E. nulan*. The alpine marsh vegetation (swamp), distributed in surface depressions, is dominated by *Kobresia tibetica* and *Podicularis longiflora*. The Haibei station was first established for ecological study in 1976, and has been part of the Chinese Ecosystem Research Network (CERN) since 1989. Numerous data of climate, soils, vegetation, animals, and livestock grazing have been accumulated over these years in the study area.

In an effort to better understand the carbon fluxes and budget of the Qinghai–Tibetan Plateau, eddy covariance flux towers were established to measure CO_2 and H_2O fluxes in the three ecosystems of the Haibei station, namely the meadow site, the swamp site, and the shrub site (Table 1). The three flux sites belong to the ChinaFLUX and AsiaFlux networks. The footprints of the flux towers are approximately 400– 450 m, depending on the height of eddy covariance system (Li et al., 2006). The half-hourly flux data are recorded at the swamp ecosystem and alpine shrub ecosystem sites, and the quarter-hourly flux data are recorded at the alpine meadow ecosystem site. The half-hourly or quarter-hourly CO_2 flux data in 2004 were used in this study.

2.2. Partitioning of NEE into gross primary production and ecosystem respiration

Daily flux data of NEE, GPP and ecosystem respiration (R) at three alpine ecosystems in 2004 were generated from the half-hourly flux data (swamp ecosystem and alpine shrub ecosystem sites) and quarter-hourly flux data (alpine meadow ecosystem site) (Fig. 1). Data quality control is implemented to reduce uncertainty. According to measurement theory of the eddy covariance technique, the half-hourly or quarter-hourly flux data were first transformed by three-dimension coordinate rotation and the WPL correction (Li et al., 2005). Then, flux values were excluded from further analysis if sensor variance was excessive, rain or snow was falling, for incomplete sample periods, or instrument malfunction. At night, the quality of flux data is often not good because of weak turbulent mixing, but the uncertainty of nighttime data could be lowered or reduced under high friction velocity ($u*$), which provides intensive turbulent mixing, so flux values were excluding from further analysis if $u*$ was below a threshold of 0.20 m/s. After the process of data quality control, the data coverage in a year was 70% for
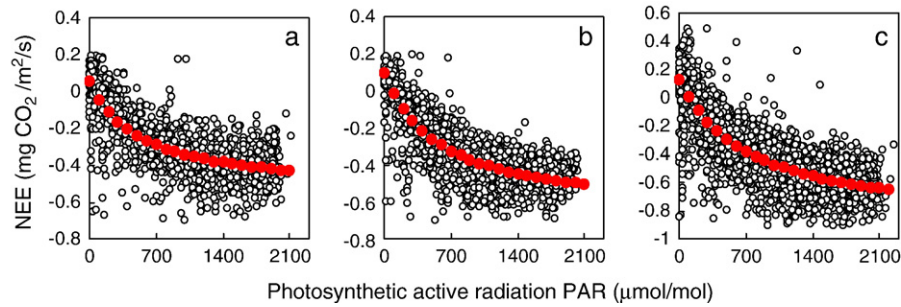
Fig. 1. The relationship between daytime net ecosystem exchange (NEE) of CO_2 and photosynthetically active radiation (PAR) in 2004 at three alpine ecosystems in Qinghai–Tibetan Plateau, China. a — swamp ecosystem, b — alpine shrub ecosystem, c — alpine meadow ecosystem.

swamp ecosystem site and 73% for alpine shrub ecosystem site, and data coverage of alpine meadow ecosystem site was 72% from April to December in 2004. To obtain annual estimates of CO_2 exchange, values missing from the half-hourly and quarter-hourly records of NEE were modeled by combining estimates of canopy photosynthesis and nocturnal respiration. Daytime CO_2 exchange rates were obtained from Michaelis–Menten models of PPFD, with coefficients fitted on a monthly basis. Missing nocturnal CO_2 exchange values were estimated from Van't Hoff function (see Eq. (1)) between air temperature and nocturnal ecosystem respiration.

$$NEE_{night} = R_{ref,10} \times Q_{10}^{(T-10)/10} \quad (1)$$

where NEE_{night} is nocturnal ecosystem respiration, $R_{ref,10}$ is ecosystem respiration on 10 °C reference temperature, Q_{10} is the change in the rate of respiration with a 10 °C change of temperature, T is air temperature near the ground.

Gap-filled half-hourly (swamp and alpine shrub sites) and quarter-hourly (alpine meadow site) NEE data were used to estimate ecosystem respiration and GPP in the following way. All data records with solar altitude less than 0 were used to estimate dark (nighttime) respiration rate. For one year, after data quality control, all observed "dark" NEE values were regressed against measured air temperature near the ground by using the Eq. (1). The relationships between nocturnal ecosystem respiration and air temperature in three alpine ecosystems are shown in Fig. 2 and Table 2. The resultant regression equation was then used with measured air temperature near the ground to predict ecosystem respiration during "light" (daytime) periods (solar altitude >0). GPP was then

estimated as NEE minus estimated ecosystem respiration for all "light" periods (using convention of opposite signs for GPP and respiration). We calculated 8-day sums of GPP and NEE from the daily GPP and NEE data, to be temporally consistent with the 8-day composite MODIS satellite images (Fig. 3, Section 2.3). We only estimated GPP of the alpine meadow ecosystem from May to October in 2004, i.e., the plant growing season.

2.3. Description of the satellite-based Vegetation Photosynthesis Model (VPM)

Based on the conceptual partitioning of chlorophyll and non-photosynthetically active vegetation (NPV) within a canopy, Xiao et al. (2004a) developed the Vegetation Photosynthesis Model (VPM) for estimation of GPP over the photosynthetically active period of vegetation. The functions used were:

$$GPP = \varepsilon_g \times FPAR_{chl} \times PAR \quad (2)$$

where $FPAR_{chl}$ is the fraction of photosynthetically active radiation (PAR) absorbed by leaf chlorophyll in the canopy, PAR is the photosynetically active radiation (μmol photosynthetic photon flux density, PPFD), and ε_g is the light use efficiency (μmol CO_2/μmol PPFD). Light use efficiency (ε_g) is affected by temperature, water, and leaf phenology:

$$\varepsilon_g = \varepsilon_0 \times T_{scalar} \times W_{scalar} \times P_{scalar} \quad (3)$$

where ε_0 is the apparent quantum yield or maximum light use efficiency (μmol CO_2/μmol PPFD), and T_{scalar}, W_{scalar} and P_{scalar} are the scalars for the effects of temperature, water and leaf phenology on light use efficiency of vegetation, respectively.
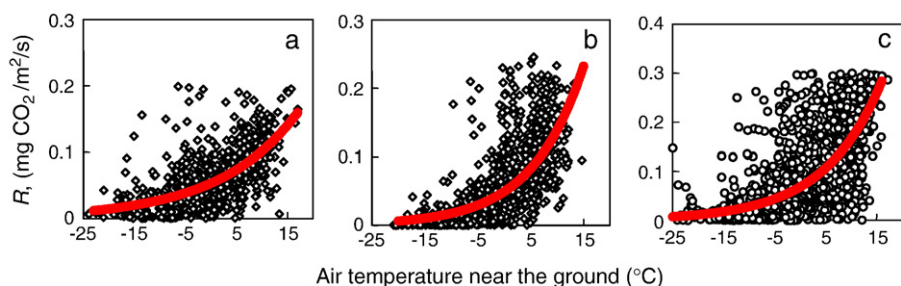
Fig. 2. Relationships between nocturnal ecosystem respiration (R) and air temperature near the ground in 2004 at three alpine ecosystems in Qinghai–Tibetan Plateau, China. a — swamp ecosystem, b — alpine shrub ecosystem, c — alpine meadow ecosystem.

Table 2
Parameters of Michaelis–Menten and Van't Hoff equation in three alpine ecosystems*

Ecosystem type	Parameters of Michaelis–Menten					Parameters of Van't Hoff				
	n	a	GEE_{max}	R^2	F-test	n	Q_{10}	$R_{ref,\,10}$	R^2	F-test
Swamp	1312	0.0014	0.6007	0.602	$p<0.001$	973	1.905	0.1017	0.4332	$p<0.001$
Shrub	1365	0.0015	0.7678	0.768	$p<0.001$	1424	2.804	0.1388	0.4842	$p<0.001$
Meadow	2943	0.0016	1.0366	0.709	$p<0.001$	1921	2.429	0.1666	0.4014	$p<0.001$

* a is maximum light use efficiency, GEE_{max} is maximum gross ecosystem exchange, $R_{ref,10}$ is ecosystem respiration on 10 °C reference temperature, Q_{10} is the change in the rate of respiration with a 10 °C change of temperature.

The full description of the VPM model is given elsewhere (Xiao, Hollinger, et al., 2004a; Xiao, Zhang et al., 2005a).

2.3.1. Vegetation indices used as input data of the VPM model

The satellite-based VPM model uses two vegetation indices as input data: Enhanced Vegetation index (EVI) and Land Surface Water Index (LSWI). The EVI and LSWI are two vegetation indices that differ from widely-used normalized difference vegetation index (NDVI). NDVI was often applied in production efficiency models to estimate vegetation productivity of terrestrial ecosystems (Field et al., 1995; Prince & Goward, 1995; Nemani et al., 2003).

$$NDVI = (\rho_{nir}-\rho_{red})/(\rho_{nir} + \rho_{red}) \qquad (4)$$

It is known that NDVI suffers several limitations, including sensitivity to atmospheric conditions, sensitivity to soil background (e.g., soil moisture), and saturation of NDVI values in multi-layered and closed canopies (Xiao et al., 2004a). With a new generation of advanced optical sensors (e.g., VGT and MODIS) coming into operation, EVI and LSWI have now been used widely to characterize the growing conditions of vegetation (Boles et al., 2004; Zhang et al., 2003).

EVI directly adjusts the reflectance in the red band as a function of the reflectance in the blue band (ρ_{blue}), accounting for residual atmospheric contamination (e.g., aerosols), variable soil and canopy background reflectance (Huete et al., 1997):

$$EVI = G \times (\rho_{nir}-\rho_{red})/(\rho_{nir} + (C_1 \times \rho_{red}-C_2 \times \rho_{blue}) + L) \qquad (5)$$

where $G=2.5$, $C_1=6$, $C_2=7.5$, and $L=1$, ρ_{nir}, ρ_{red} and ρ_{blue} is reflectance of blue, red and near infrared bands.

As the short infrared (SWIR) spectral band is sensitive to vegetation water content and soil moisture, a combination of NIR and SWIR bands have been used to derive water sensitive vegetation indices (Ceccato, Flasse et al., 2001, 2002; Ceccato, Gobron, et al., 2002a; Xiao et al., 2004a). LSWI is calculated as the normalized difference between NIR and SWIR spectral bands (Xiao et al., 2002):

$$LSWI = (\rho_{nir}-\rho_{swir})/(\rho_{nir} + \rho_{swir}) \qquad (6)$$

where ρ_{nir} and ρ_{swir} is reflectance of near infrared bands and short infrared bands.

The MODIS sensor onboard the NASA Terra satellite has 36 spectral bands. Seven spectral bands are primarily designed for the study of vegetation and land surface: blue (459–479 nm), green (545–565 nm), red (620–670 nm), near infrared (841–875 nm, 1230–1250 nm) and shortwave infrared (1628–1652 nm, 2105–2155 nm). In this study we downloaded the 8-day Land Surface Reflectance (MOD09A1) data sets from the EROS Data Center, US Geological Survey (http://www.edc.usgs.gov/). Reflectance values of these four spectral bands (blue, red, near infrared (841–875 nm), shortwave infrared (1628–1652 nm)) in 2004 were used to calculate vegetation indices (NDVI, EVI and LSWI). The extent of flux towers footprints (400–450 m) was approximately equal to the size of one MODIS pixel, and the field survey and Landsat image analysis show that the land surface surrounding the flux towers is characterized as homogeneous surface. An earlier study discussed the reliability of using one MODIS pixel, 3×3 MODIS pixels and 5×5 MODIS pixels for analysis of vegetation indices and simulation of the VPM model at a forest eddy flux tower site (Xiao et al., 2005a). In
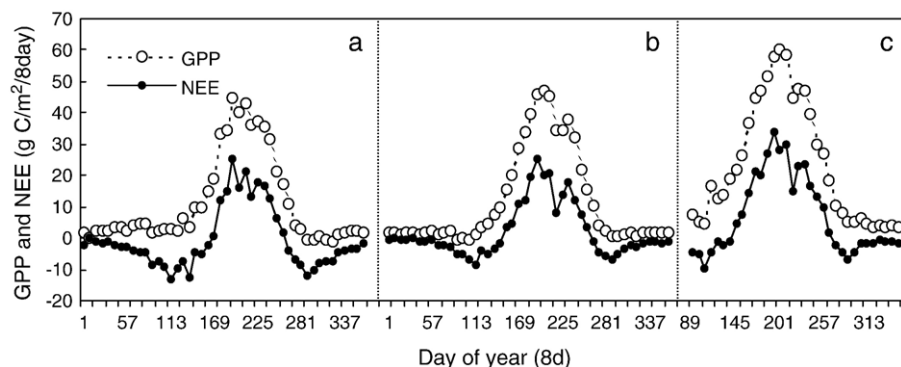
Fig. 3. The seasonal dynamics of net ecosystem exchange of CO_2 (NEE), and gross primary production (GPP) in 2004 at three alpine ecosystems in Qinghai–Tibetan Plateau, China. a — swamp ecosystem, b — alpine shrub ecosystem, c — alpine meadow ecosystem.
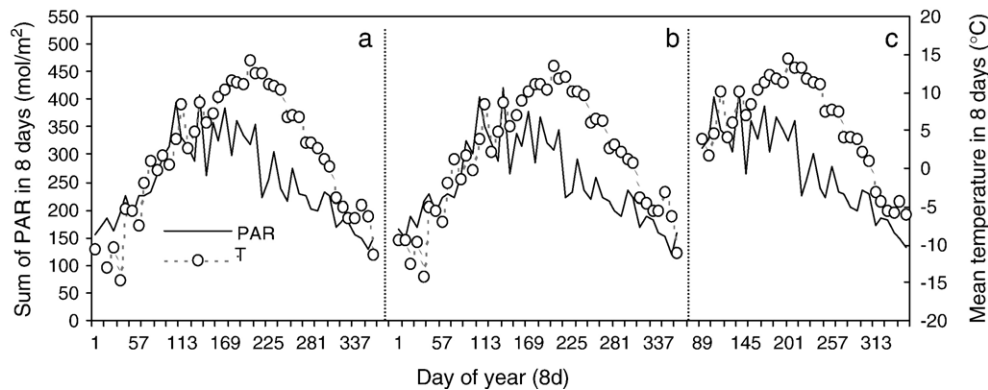
Fig. 4. The seasonal dynamics of PAR and mean air temperature (T) during 2004 at three alpine ecosystems in Qinghai–Tibetan Plateau, China. a — swamp ecosystem, b — alpine shrub ecosystem, c — alpine meadow ecosystem.

this study, the times series data of site-specific vegetation indices in 2004 were extracted from one MODIS pixel that is centered on the flux tower, based on the geo-location information (latitude and longitude) of the flux tower sites.

2.3.2. Estimating canopy-level maximum light use efficiency (ε_0) parameter

In the VPM model, the ecosystem-level ε_0 values vary with vegetation type. Information about ε_0 for individual vegetation types can be obtained from analysis of net ecosystem exchange (NEE) of CO_2 and incident PAR ($\mu mol/m^2/s$ photosynthetic photon flux density) at CO_2 eddy flux tower sites (Goulden et al., 1997). In order to obtain the ε_0 values of alpine meadow, swamp and alpine shrub, we had estimated the nonlinear model between NEE and PAR by using the Michaelis–Menten function (Eq. (7)), based on the data within the peak period of vegetation growing season (from July to August) in 2004. The fit curves and regression parameters of the Michaelis–Menten function were shown in Fig. 1 and Table 2.

$$NEE = \frac{\alpha \times PPFD \times GEE_{max}}{\alpha \times PPFD + GEE_{max}} - R \qquad (7)$$

where α is maximum light use efficiency or apparent quantum yield (as PPFD approaches to 0), PPFD is photosynthetic photon flux density, GEE_{max} is maximum gross ecosystem exchange, R is ecosystem respiration. The estimated α value is used as an estimate of the ε_0 parameter in the VPM model.

2.3.3. Estimating parameters for temperature, water and phenological down-regulation scalars

Detailed descriptions of the functions of calculating T_{scalar}, W_{scalar} and P_{scalar} (see Eq. (3)) are presented in earlier publications (Xiao et al., 2004a). In calculation of T_{scalar} (see Xiao et al., 2004a), T_{min}, T_{opt} and T_{max} values vary among different vegetation types. For the three alpine ecosystems in this study, we use 0, 20 and 35 °C for T_{min}, T_{opt} and T_{max}, respectively, based on the relationship between temperature and photosynthesis, and the analysis of VPM model testing. Photosynthesis of alpine ecosystems is often limited by low temperature. To better capture the effect of air temperature on

photosynthesis, in the calculation of T_{scalar}, we used the average daytime temperature during light periods (solar altitude >0), instead of using the daily mean air temperature that is calculated as the average value between daily maximum temperature (generally daytime) and daily minimum temperature (night time).

Estimation of site-specific $LSWI_{max}$ is dependent upon the time series of remote sensing data. The maximum LSWI value within the plant-growing season was selected as an estimate of $LSWI_{max}$ (Xiao, Hollinger et al., 2004a; Xiao, Zhang et al., 2004b; Xiao, Zhang, Hollinger et al., 2005a; Xiao, Zhang, Saleska et al., 2005b). Based on the analysis of LSWI seasonal dynamics derived from MODIS image data from 2003 to 2004, we used 0.30 for $LSWI_{max}$ of swamp ecosystem and alpine shrub ecosystem, and used 0.32 for $LSWI_{max}$ of alpine meadow ecosystem. As a grassland canopy has new leaves emerging throughout much of the plant growing season, P_{scalar} is set to 1.0 in this study.

3. Results

3.1. Seasonal dynamics of NEE and GPP in 2004

Fig. 3 shows that the NEE and GPP time series in 2004 at the three alpine ecosystems had distinct seasonal cycles. The seasonal dynamics of GPP can be explained in part by the seasonal dynamics of air temperature and PAR (Fig. 4). In winter season (day of year—DOY—ranging from 1 to 120 and from 300 to 365), because low air temperature and frozen soils inhibit photosynthetic activities of the alpine ecosystems, GPP values were near zero and NEE were mostly dominated by ecosystem respiration. From DOY 120 of 2004 as PAR intensified and air temperature went over the limit of minimum temperature of photosynthetic activities, the vegetation began to grow and ecosystem photosynthesis capability gradually increased, GPP also began to increase and reached its peak during DOY 180–240. Later on GPP declined gradually as temperature declined and vegetation started to wither. Photosynthetic capability of the three alpine ecosystems differed in 2004. The alpine meadow had the highest photosynthetic capability, as its peak and total value of GPP during the growing season (from May to October) was 67.7 g C/m²·8 days and
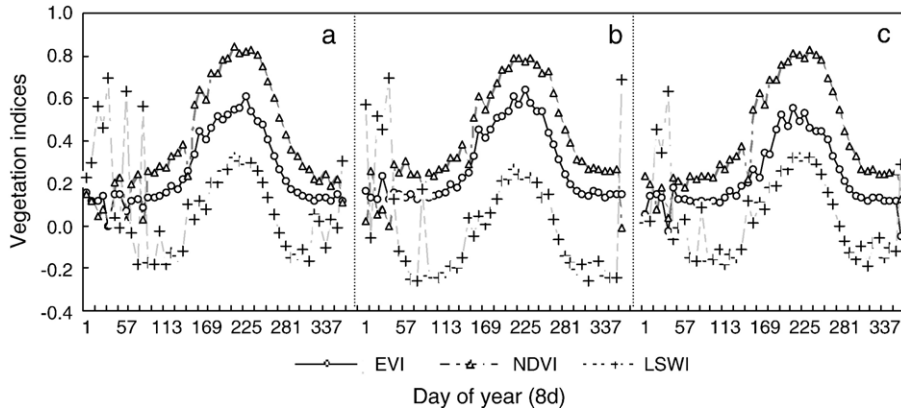
Fig. 5. The seasonal dynamics of EVI, LSWI and NDVI in 2004 at three alpine ecosystems in Qinghai–Tibetan Plateau, China. a — swamp ecosystem, b — alpine shrub ecosystem, c — alpine meadow ecosystem.

733.0 g C/m^2, respectively. The peak and total value of GPP during the plant growing season were approximately 46.8 g C/ m^2, and 496.5 g C/m^2 at the alpine shrub. The photosynthesis capability of the swamp was the smallest, with a peak GPP value of 44.8 g C/m^2, and a total GPP value of 465.5 g C/m^2 in the plant growing season, respectively.

3.2. Seasonal dynamics of site-specific vegetation indices

Fig. 5 shows that EVI, NDVI and LSWI of the three alpine ecosystems had strong seasonal dynamics. The vegetation indices derived from MODIS data captured the beginning and ending of the plant growing season well in 2004. The EVI and NDVI began an abrupt increase on DOY 120 and reached their

peak value during DOY 201–249, then they started to decline gradually and remained low after DOY 300. In the winter months (December, January and February), LSWI values were high, which was attributed to snow cover (Fig. 5). As snow melted in the spring (March and April), LSWI declined gradually. The LSWI time series data had a seasonal cycle with a spring trough and a fall trough, which can be easily recognized from analysis of LSWI time series data.

3.3. Temporal correlation between vegetation indices and GPP

The seasonal dynamics of GPP were well-correlated with that of the vegetation indices (NDVI and EVI, Fig. 6). During winter periods (DOY 1–120 and 300–365), the two vegetation
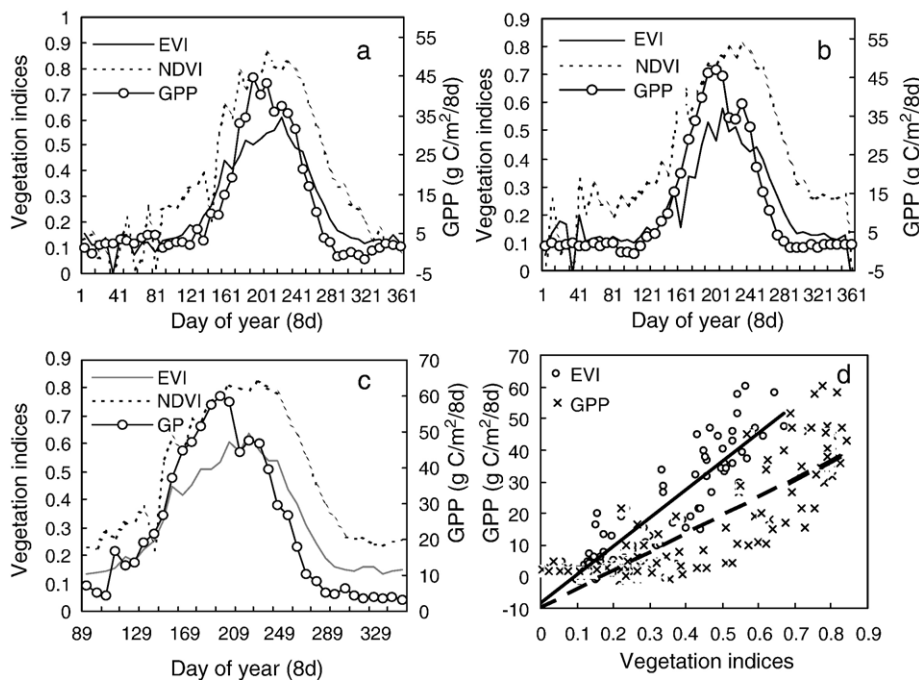
Fig. 6. Comparison between vegetation indices (EVI, NDVI) and gross primary production (see Fig. 3) at the three flux tower sites, a — swamp ecosystem, b — alpine shrub ecosystem, c — alpine meadow ecosystem. d — Simple linear regression analyses between GPP and vegetation indices (NDVI, EVI), with data for all three sites combined. Solid line is regression analysis between GPP and EVI (GPP = 90.20EVI − 8.59, R^2 = 0.85), and dashed line is regression analysis between GPP and NDVI (GPP = 58.53NDVI − 9.88, R^2 = 0.73).
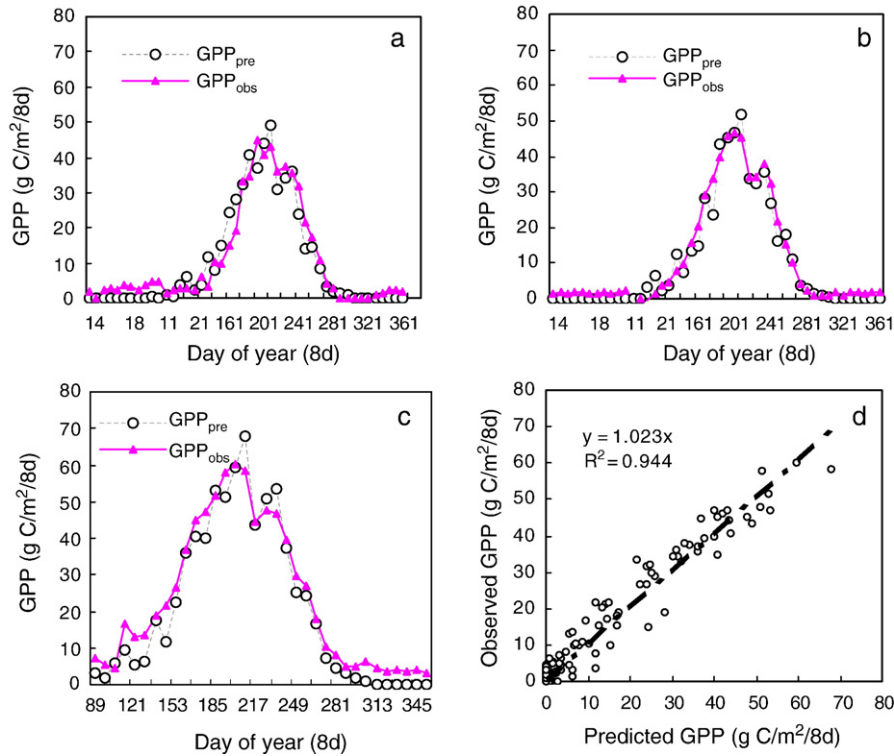
Fig. 7. Comparison of the seasonal dynamics between the observed gross primary production (GPP) and predicted GPP in 2004 at three eddy flux tower sites. a — swamp ecosystem, b — alpine shrub ecosystem, c — alpine meadow ecosystem. d — Simple linear regression analysis between the observed GPP and predicted GPP, with data for all three sites combined.

indices were at low levels and GPP values were near zero because of no vegetation photosynthesis in winter. From DOY 120 the two vegetation indices and GPP of ecosystems gradually increased as vegetations grew and reached their peaks during DOY 180–240. However, the seasonal dynamics of EVI differs from that of NDVI in terms of both magnitude and phase. During the plant growing season, the maximum NDVI value ranges in the order of 0.75–0.85, and were much higher than the maximum EVI values (in the order of 0.5–0.6). Although the dynamic variations of EVI and NDVI both lagged behind those of GPP during vegetation grow peaks, EVI followed GPP better than NDVI, especially in alpine shrub ecosystem (Fig. 6b). When using all the observations of the three alpine ecosystems in 2004, EVI has a stronger linear relationship with GPP than NDVI does (Fig. 6d). This result was consistent with the previous studies (Xiao, Hollinger et al., 2004a; Xiao, Zhang et al., 2004b).

3.4. Simulations of the VPM model

The VPM model was run at 8-day time scale using the site-specific data of temperature, PAR and vegetation indices in 2004. The seasonal dynamics of predicted GPP (GPP$_{pre}$) from the VPM model was compared with the observed GPP (GPP$_{obs}$) data (Fig. 7). There exist discrepancies between GPP$_{obs}$ and GPP$_{pre}$ in a few 8-day periods; for instance, many GPP$_{pre}$ values are lower than GPP$_{obs}$ values, especially in alpine meadow ecosystem and alpine shrub ecosystem. Occasionally, GPP$_{pre}$

values are higher than GPP$_{obs}$ at the peak of the growing season. Generally, the predicted GPP by the VPM model agreed well with estimated GPP from the flux towers data in the three alpine ecosystems. The seasonal dynamics of GPP$_{pre}$ matched reasonably well with those of GPP$_{obs}$, and the simple linear regression model also shows a good agreement between GPP$_{pre}$ and GPP$_{obs}$ (Fig. 7d). Seasonally integrated GPP$_{pre}$ over the period of May to October (plant-growing season) was only slightly lower than seasonally integrated GPP$_{obs}$, ranging from 1.4% to 7.4%, and the annual GPP$_{pre}$ was lower than annual GPP$_{obs}$, 6.2% in swamp ecosystem and 8.2% in alpine shrub ecosystem (Table 3).

Table 3
Comparison between the observed GPP and predicted GPP in three alpine ecosystems (g C/m^2)*

Ecosystem type	Flux tower data		VPM model	
	GPP$_{obs(5-10)}$	GPP$_{obs(1-12)}$	GPP$_{pre(5-10)}$	GPP$_{pre(1-12)}$
Swamp	465.5	508.6	459.0 (RE=1.4%)	476.9 (RE=6.2%)
Alpine shrub	496.5	528.8	473.4 (RE=4.7%)	485.7 (RE=8.2%)
Alpine meadow	733.0	789.2 (From Apr to Dec)	678.8 (RE=7.4%)	696.1 (From Apr to Dec)

* GPP$_{obs(1-12)}$ and GPP$_{pre(1-12)}$ are the observed and predicted annual GPP from January to December, respectively. GPP$_{obs(5-10)}$ and GPP$_{pre(5-10)}$ are seasonally integrated sums of the observed GPP and predicted GPP over the period of May 1 to October 31, respectively. RE=[(GPP$_{obs}$−GPP$_{pre}$)/GPP$_{obs}$]×100%.

4. Discussion and summary

As the leaf phenological cycle (leaf flush, expansion, senescence, fall) progresses, canopy leaves change in their biophysical, biochemical (e.g., chlorophyll and other pigments, nitrogen) and optical properties, which in turn influence both biophysical parameters (e.g., albedo, latent and sensible heat flux) and biogeochemical parameters (e.g., photosynthesis) of the land surface (Xiao et al., 2004b). Limited studies had evaluated radiometric and biophysical performance of vegetation indices (EVI, NDVI) from MODIS data (Huete et al., 2002). In this study, we evaluated the biophysical performance of vegetation indices (NDVI and EVI) in relation to GPP of three alpine ecosystems in Qinghai–Tibetan Plateau, China. The quantitative relationships between the vegetation indices and CO_2 flux data clearly demonstrated the improvement of EVI over NDVI, in terms of the phase and magnitude of photosynthesis. And the time series of EVI and LSWI provided valuable insight into the processes (e.g., growing season length and water condition) that regulate ecosystem carbon exchange. These sensor-specific advanced vegetation indices (e.g. EVI and LSWI) have been optimized for the Moderate Resolution Imaging Spectroradiometer (MODIS), the Global Imager (GLI) and the VEGETATION sensors. Clearly, there is a need to examine those advanced vegetation indices in relation to leaf phenology and the seasonal dynamics of GPP across the flux tower sites in various biomes.

The simulation results of the VPM model have shown that predicted GPP agreed well with observed GPP of the three alpine ecosystems in Qinghai–Tibetan Plateau. The results from this study and earlier VPM studies of forest (Xiao, Hollinger et al., 2004a; Xiao, Zhang et al., 2004b, 2005b) indirectly support the Chlorophyll–$FPAR_{chl}$–EVI hypotheses and leaf water-LSWI hypothesis implemented in the VPM model. The VPM model is an alternative, complementary to other production efficiency models that are based on the LAI–$FPAR_{canopy}$–NDVI paradigm. Recently, the standard MODIS-based GPP estimates (8-day composite) from the MODIS-PSN algorithm (Running et al., 2000) which built upon the LAI–$FPAR_{canopy}$–NDVI relationships become available to the public, and the BigFoot project has evaluated MODIS standard GPP and NPP products (MOD17), relying on running the Biome-BGC model (Turner et al., 2005). The study results of Turner et al. (2005) indicated that the GPP predicted by the PSN did not match well with tower-based GPP with regard to the beginning and end of the growing season at the desert grassland site (SEVI). Moreover, the phase of MODIS-based GPP significantly deviated from that of tower-based GPP in the period of from about DOY 60 to DOY 200. Combining information on the phenomenology of relationships of grassland GPP with photosynthetically active radiation, NDVI, and soil water, Gilmanov et al. (2005) used the empirical model to estimate GPP of grassland (Mandan site) at 10-day time scale. According to the simple linear regression analysis between GPP_{obs} and GPP_{pre}, the simulated GPP_{pre} by the empirical model accounts for 68% ($R^2 = 0.68$) of the variance in GPP_{obs} (Gilmanov et al., 2005). In this study, the phase and magnitude of GPP estimated by the VPM model was very consistent with

tower-based GPP ($R^2 = 0.94$, see Fig. 7d). Further comparison between the VPM model and other GPP models across various CO_2 eddy flux tower sites is needed in the future.

Among simulation results of the VPM model, there still exist differences between GPP_{pred} and GPP_{obs} for a few 8-day periods (Fig. 7), accounting for most of the differences between seasonally integrated GPP_{obs} and GPP_{pred} (Table 3). Those discrepancies between GPP_{obs} and GPP_{pre} may be attributed to three sources of errors. The first source is the sensitivity of the VPM model to PAR and temperature, for instance, smaller GPP_{pre} in DOY 113–145 at alpine meadow ecosystem and in DOY 161–169 at alpine shrub ecosystem, and larger GPP_{pre} in DOY 161–177 at swamp ecosystem. The second source is the time-series data of vegetation indices derived from satellite images. We used the 8-day MODIS composite images that have no BRDF correction or normalization, and thus, the effect of angular geometry on surface reflectance and vegetation indices remained. The third source is the error (overestimation or underestimation) of the observed GPP (GPP_{obs}). GPP_{obs} is calculated from flux-measured NEE and estimated daytime ecosystem respiration. The two major steps that must be taken to calculate GPP are the gap filling of NEE and estimation of daytime (solar altitude > 0) ecosystem respiration. Both of these steps require subjective decisions and are currently the subject of a great deal of discussion (Falge, Baldocchi, et al., 2002a, Falge, Tenhunen et al., 2002b). On the other hand, in winter, there was an illusive phenomenon that flux-measured NEE had a few negative values, indicating that vegetation was still photosynthesizing. Actually, there was no green vegetation present. This phenomenon resulted in annual GPP_{obs} calculated from flux towers data being larger than GPP_{pre} of the VPM model in the three ecosystems, especially in swamp ecosystem and alpine meadow ecosystem.

The light use efficiency (ε_g) is the basis for the Production Efficiency Models (PEMs), and the accurate estimating of ε_g is one of key steps for using the PEMs to estimate either GPP or NPP (Running et al., 1999). In natural ecosystems, ε_g is determined by many biological and biophysical factors as well as environmental factors. Much attention should be given to the variability of ε_g among vegetation types across a heterogeneous landscape. If ε_g differs significantly among vegetation types, these differences should be accounted for when estimating GPP with remotely sensed data. The eddy covariance technique provides a significant potential approach to estimate the canopy-level ε_g (Turner et al., 2003), and now over 300 CO_2 eddy flux tower sites in the world constitute a global FLUXNET network (http://www.fluxnet.ornl.gov/fluxnet/index.cfm). In this study, we used CO_2 flux data to estimate the canopy-level maximum light use efficiency (ε_0), which is complementary to the literature survey approach used in previous VPM studies (Xiao, Hollinger et al., 2004a; Xiao, Zhang et al., 2004b; Xiao, Zhang, Hollinger et al., 2005a; Xiao, Zhang, Saleska et al., 2005b). Although the scatter plots of NEE and PAR showed some degree of data scattering, owing to the changes in environmental factors (Fig. 1), the fits for Michaelis–Menten were statistically significant at the F-test of 0.01 level (Table 2). As more CO_2 flux data of FLUXNET sites become available, a

mega-data analysis of CO_2 fluxes will help estimate ε_0 across various vegetation types. Combining vegetation indices (EVI, LSWI), climate data (PAR, temperature) and maximum light use efficiency (ε_0) parameter for individual vegetation types, the VPM model is capable for estimating regional or global GPP. The uncertainty of regional estimation of the VPM model will be assessed in further studies.

In summary, we have used net CO_2 exchange flux data of three alpine ecosystems in Qinghai–Tibetan Plateau to estimate parameters of the VPM model and simulated the seasonal dynamics of GPP of three alpine ecosystems by integrating climate data and MODIS vegetation indices with the VPM model. These results indicate that the seasonal dynamics of GPP predicted by the VPM model matched well with observed GPP from eddy flux towers. The predicted annual GPP values agreed reasonably well with observed annual GPP, with 7.2% mean relative error. Moreover, the mean relative error of the cumulative GPP was only 4.4% between the predicted and observed in the plant growth season (from May to October). And the results have demonstrated that EVI had a stronger linear relationship with GPP than did NDVI. This study also highlighted the biophysical performance of improved vegetation indices in relation to GPP and demonstrated the potential of the VPM model for scaling-up of GPP of alpine grassland ecosystems. Additional studies are needed to validate the capability of the VPM model in capturing the interannual GPP variations of alpine grassland ecosystems, as additional CO_2 flux data become available in the near future.

Acknowledgments

References

Aalto, T., Ciais, P., & Chevillard, A. (2004). Optimal determination of the parameters controlling biospheric CO_2 fluxes over Europe using eddy covariance fluxes and satellite NDVI measurements. *Tellus*, 56B, 93−104.

Behrenfeld, M. J., Randerson, J. T., McClain, C. R., Feldman, G. C., Los, S. O., Tucker, C. J., et al. (2001). Biospheric primary production during an ENSO transition. *Science*, 291, 2594−2597.

Boles, S., Xiao, X., Liu, J., Zhang, Q., Munkhutya, S., Chen, S., & Ojima, D. (2004). Land cover characterization of temperate East Asia: Using multi-temporal image data of VEGETATION sensor. *Remote Sensing of Environment*, 90(4), 477−489.

Ceccato, P., Flasse, S., & Gregoire, J. M. (2002). Designing a spectral index to estimate vegetation water content from remote sensing data: Part 2. Validation and applications. *Remote Sensing of Environment*, 82, 198−207.

Ceccato, P., Flasse, S., Tarantola, S., Jacquemoud, S., & Gregoire, J. M. (2001). Detecting vegetation leaf water content using reflectance in the optical domain. *Remote Sensing of Environment*, 77, 22−33.

Ceccato, P., Gobron, N., Flasse, S., Pinty, B., & Tarantola, S. (2002). Designing a spectral index to estimate vegetation water content from remote sensing data: Part 1. Theoretical approach. *Remote Sensing of Environment*, 82, 188−197.

Falge, E., Baldocchi, D., Tenhunen, J., Aubinet, M., Bakwin, P., Berbigier, P., et al. (2002). Seasonality of ecosystem respiration and gross primary production as derived from FLUXNET measurements. *Agricultural and Forest Meteorology*, 113, 53−74.

Falge, E., Tenhunen, J., Baldocchi, D., Aubinet, M., Bakwin, P., Berbigier, P., et al. (2002). Phase and amplitude of ecosystem carbon release and uptake potentials as derived from FLUXNET measurements. *Agricultural and Forest Meteorology*, 113, 75−95.

Field, C. B., Behrenfeld, M. J., Randerson, J. T., & Falkowski, P. (1998). Primary production of the biosphere: Integrating terrestrial and oceanic components. *Science*, 281, 237−240.

Field, C. B., Randerson, J. T., & Malmstrom, C. M. (1995). Global net primary production-combining ecology and remote sensing. *Remote Sensing of Environment*, 51, 74−88.

Gilmanov, T. G., Tieszen, L. L., Wylie, B. K., Flanagan, L. B., Frank, A. B., Haferkamp, M. R., et al. (2005). Integration of CO_2 flux and remotely-sensed data for primary production and ecosystem respiration analyses in the Northern Great Plains: Potential for quantitative spatial extrapolation. *Global Ecology and Biogeography*, 74−88.

Goulden, M. L., Daube, B. C., Fan, S. M., Sutton, D. J., Bazzaz, A., Munger, J. W., et al. (1997). Physiological responses of a black spruce forest to weather. *Journal of Geophysical Research-Atmospheres*, 102, 28987−28996.

Huete, A., Didan, K., Miura, T., Rodriguez, E. P., Gao, X., Ferreira, L. G., et al. (2002). Overview of the radiometric and biophysical performance of the MODIS vegetation indices. *Remote Sensing of Environment*, 83, 195−213.

Huete, A. R., Liu, H. Q., Batchily, K., & vanLeeuwen, W. (1997). A comparison of vegetation indices over a global set of TM images for EOS-MODIS. *Remote Sensing of Environment*, 59, 440−451.

Li, Z. Q., Yu, G. R., Li, Q. K., Fu, Y. L., & Li, Y. N. (2006). Effect of spatial variation on areal evapotranspiration simulation in Haibei, Tibet plateau, China. *International Journal of Remote Sensing*, 27, 3487−3498.

Li, Z. Q, Yu, G. R., Wen, X. F., Zhang, L. M., Ren, C. Y., & Fu, Y. L. (2005). Energy balance closure at ChinaFLUX sites. *Science in China. Series D, Earth Science*, 48, 51−62 (Supp).

Nemani, R. R., Keeling, C. D., Hashimoto, H., Jolly, W. M., Piper, S. C., Tucker, C. J., et al. (2003). Climate-driven increases in global terrestrial net primary production from 1982 to 1999. *Science*, 1560−1563.

Oechel, W., Vourlitis, G., Verfaillliejr, J., Crawford, T., Brooks, S., Dumas, E., et al. (2000). A scaling approach for quantifying the net CO_2 flux of the Kuparuk River Basin, Alaska. *Global Change Biology*, 6(Suppl. 1), 160−173.

Osmond, B., Ananyev, G., Berry, J., Langdon, C., Kolber, Z., Lin, G., et al. (2004). Changing the way we think about global change research: Scaling up in experimental ecosystem science. *Global Change Biology*, 10, 393−407.

Prince, S. D., & Goward, S. N. (1995). Global primary production: A remote sensing approach. *Journal of Biogeography*, 22, 815−835.

Ruimy, A., Kergoat, L., & Bondeau, A. (1999). Comparing global models of terrestrial net primary productivity (NPP): Analysis of differences in light absorption and light-use efficiency. *Global Change Biology*, 5, 56−64.

Running, S. W., Baldocchi, D. D., Turner, D. P., Gower, S. T., Bakwin, P. S., & Hibbard, K. A. (1999). A global terrestrial monitoring network integrating tower fluxes, flask sampling, ecosystem modeling and EOS satellite data. *Remote Sensing of Environment*, 70, 108−127.

Running, S. W., Thornton, P. E., Nemani, R., & Glassy, J. M. (2000). Global terrestrial gross and net primary productivity from the Earth Observing System. In O. E. Sala, R. B. Jackson, & H. A. Mooney (Eds.), *Methods in Ecosystem Science*, (pp. 44−57). New York: Springer.

Turner, D. P., Ritts, W. D., Cohen, W. B., Gower, S. T., Zhao, M. S., Running, S. W., et al. (2003). Scaling Gross Primary Production (GPP) over boreal and deciduous forest landscapes in support of MODIS GPP product validation. *Remote Sensing of Environment*, *88*, 256−270.

Turner, D. P., Ritts, W. D., Cohen, W. B., Maeirsperger, T., Gower, S., Kirschbaum, A., et al. (2005). Site-level evaluation of satellite-based global terrestrial gross primary production and net primary production monitoring. *Global Change Biology*, *11*, 666−684.

Xiao, X., Boles, S., Liu, J. Y., Zhuang, D. F., & Liu, M. L. (2002). Characterization of forest types in Northeastern China, using multi-temporal SPOT-4 VEGETATION sensor data. *Remote Sensing of Environment*, *82*, 335−348.

Xiao, X. M., Hollinger, D., Aber, J. D., Goltz, M., Davidson, E. A., & Zhang, Q. Y. (2004). Satellite-based modeling of gross primary production in an evergreen needle leaf forest. *Remote Sensing of Environment*, *89*, 519−534.

Xiao, X. M., Zhang, Q., Braswell, B., Urbanski, S., Boles, S., Wofsy, S. C., et al. (2004). Modeling gross primary production of temperate deciduous broadleaf forest using satellite images and climate data. *Remote Sensing of Environment*, *91*, 256−270.

Xiao, X. M., Zhang, Q. Y., Hollinger, D., Aber, J., & Moore, B. (2005). Modeling gross primary production of an evergreen needleleaf forest using MODIS and climate data. *Ecological Applications*, *15*, 954−969.

Xiao, X. M., Zhang, Q. Y., Saleska, S., Hutyra, L., Camargo, P. D., Wofsy, W., et al. (2005). Satellite-based modeling of gross primary production in a seasonally moist tropical evergreen forest. *Remote Sensing of Environment*, *94*, 105−122.

Yu, G. R., Zhang, L. M., Sun, X. M., Fu, Y. L., & Li, Z. Q. (2005). Advances in carbon flux observation and research in Asia. *Science in China. Series D, Earth Science*, *48*, 1−16 (Supp).

Zhang, X. Y., Friedl, M. A., Schaaf, C. B., Strahler, A. H., Hodges, J. C. F., Gao, F., et al. (2003). Monitoring vegetation phenology using MODIS. *Remote Sensing of Environment*, *84*, 471−475.

Zhao, X. Q., & Zhou, X. M. (1999). Ecological basis of alpine meadow ecosystem management in Tibet: Haibei alpine meadow ecosystem research station. *Ambio*, *28*(8), 642−647.